

Assessing Effects of Rate Parameter Changes on Ozone Models Using Sensitivity Analysis[†]

Gregory P. Smith*

Molecular Physics Laboratory, SRI International, Menlo Park, California 94025

Manvendra K. Dubey

Atmospheric and Climate Sciences, Los Alamos National Laboratory, Los Alamos, New Mexico 87545

Douglas E. Kinnison

National Center for Atmospheric Research, Boulder, Colorado 80307

Peter S. Connell

*Lawrence Livermore National Laboratory, Livermore, California 94550**Received: June 30, 2000; In Final Form: September 22, 2000*

Effects of recommended rate parameter changes in the NASA JPL-2000 evaluation from JPL-94 values on local ozone concentrations in a 2-D model are predicted using local sensitivity analysis results from the LLNL 2-D diurnally averaged model. Ozone decreases of 5% in the middle stratosphere and 10% increases near the tropopause and upper troposphere are indicated. Altered NO_x kinetics are largely responsible for these changes, and increased model NO_x levels and ozone depletion from stratospheric aircraft are also expected according to sensitivity analysis. Effects of specific changes, such as the nitric acid formation rate, are examined. New error bars on rate parameters in the evaluation are propagated by the sensitivity coefficients to derive revised kinetics uncertainties for the model ozone calculations at several altitudes, latitudes, and seasons. Middle-upper stratospheric ozone uncertainties of 12% from the catalytic photochemistry are indicated, increasing in the lower stratosphere.

Introduction

Coupled photochemical–dynamical models of the atmosphere are relied upon to assess effects of anthropogenic and natural variations on ozone. Recent complex assessment studies¹ of the effects from a proposed supersonic aircraft (SST) fleet are one such case, refining the pioneering work of Johnston² which sounded the alert to ozone depletion by stratospheric NO_x emissions. Other examples include halogen-induced global stratospheric ozone depletion, the polar ozone holes, effects from volcanic eruptions, and climate change from alterations of atmospheric composition. One of the largest sources of uncertainty in such model-based predictions stems from the uncertainties in the kinetic and photolysis rate parameters for more than 150 individual steps in the chemical mechanism. Two evaluation panels^{3,4} provide regular reports to the community, to minimize this error source and furnish a uniformity in this modeling input. New measurements and reevaluations result in periodic revisions of the recommended values for some of the key parameters, as well as narrowing the estimated error bars. The JPL-2000 edition from the NASA evaluation panel³ is the most recent example. When such progress occurs, the modeler and reader face the question of how previous results are affected and whether studies must be repeated. Historically, improvements in the mechanism and rate parameters have had some significant effects on ozone assessment predictions, on occasion even altering the direction of predicted ozone change from SST fleets.¹

In addition, the mechanism and model are repeatedly being tested by atmospheric observations.⁵ These data with modeling interpretation can either validate the photochemical mechanism, suggest changes or adjustments, or narrow the above-mentioned error limits and provide increased confidence in model predictions. Again, if either new basic rate measurements or changes suggested from observation are proposed for adoption, the question of effects and errors in model runs remains.

This issue of how model ozone results are altered if a new set of rate parameters is adopted is by definition a sensitivity coefficient problem. The sensitivity coefficient S is the ratio of the relative change in a predicted model concentration with respect to a relative change in a model rate parameter:

$$S_i(\text{O}_3) = \partial[\text{O}_3]/[\text{O}_3]/\partial k_i/k_i = \partial(\ln[\text{O}_3])/\partial(\ln k_i) \quad (1)$$

Here k_i is the i th rate constant. Modern kinetics integrators for dimensionless problems can compute these values routinely. It is then straightforward to compute a predicted effect for a group of rate parameter changes δk_i to the final concentration, without repeating the entire calculation:

$$\Delta[\text{O}_3]/[\text{O}_3] = \sum S_i(\text{O}_3)(\delta k_i/k_i) \quad (2)$$

In addition laboratory uncertainties from individual steps σk_j can be propagated (added in quadrature) to get a measure of the overall photochemical uncertainty U in model predictions:

$$U(\text{O}_3) = (\sum (S_j \times \sigma k_j/k_j)^2)^{1/2} \quad (3)$$

[†] Part of the special issue “Harold Johnston Festschrift”.

We recently computed a set of localized sensitivity coefficients for ozone⁶ at a variety of locations in the LLNL 2-D atmospheric photochemical model,⁷ using a box model approach to freeze the solution while calculating the sensitivities. This paper uses these sensitivities to propagate the rate parameter changes of JPL-2000 into predicted 2-D model ozone changes at various locations, thus examining some of the implications of the revisions. The sensitivities allow one to approximately compute the effects of such changes without new 2-D simulations. Significant ozone and NO_x changes are indicated below 35 km, largely due to revised rate constants for O + NO₂, OH + NO₂, and OH + HNO₃. These changes also affect predicted high altitude aircraft effects on ozone. Some effects of other changes are also presented. The sensitivities are used to provide total kinetics uncertainty estimates for ozone as well. We note that Kohlmann et al.⁸ recently examined effects of updated rate parameters on tropospheric box model concentrations.

Method

Our approach is to form a 0-D box model of each location in the diurnally averaged LLNL 2-D chemical-radiative-transport model⁷ and to compute the gradient of all model species with respect to all mechanism rate parameters directly in a box model run using the Senkin code.⁹ This well-tested, sequential, finite-difference, back-substitution algorithm was developed for stiff combustion chemistry problems by Sandia National Laboratories. Tight tolerances are imposed for high accuracy. The time scales of the implicitly included kinetics range from seconds to decades, over 10 orders of magnitude, resulting in a very stiff set of differential equations. The Senkin code performs admirably and routinely in solving such problems. The sensitivity coefficient represents the time propagation of an infinitesimal perturbation of a rate parameter. Individual sensitivities converge after an initial growth period on a time scale of that specific process. All local, first-order sensitivity coefficients are computed as functions of time for all species with respect to all rate processes, in a very efficient manner. Since the Senkin package requires a fixed set of mechanism parameters, it is applied to instantaneous and localized snapshots of the 2-D model. The local nature of this direct sensitivity analysis does necessitate a careful box analysis of the 2-D stratospheric model, as elaborated below and in an LLNL report.⁶ We have used this approach previously to examine kinetics uncertainties in assessment models of aircraft effects on stratospheric ozone¹⁰ and the role of the reactions OH + ClO → HCl + O₂¹¹ and OH + NO₂ ↔ HOONO.¹² The caveats include that feedbacks from transport, radiative, and large chemical changes in nearby boxes or from seasonality are not included in our local-linear analyses. Nonlinearities from large rate constant changes can also be missed by the analysis.

Local sensitivity calculations of the 2-D LLNL model by the Senkin package pose several challenges and some constraints. A series of 0-D parcels with diurnally averaged parameters have to be routinely extracted from the exhaustive 2-D model output. Since sensitivity coefficients represent the time-dependent propagation of infinitesimal perturbations in rate parameters, individual sensitivities grow and converge on the time scale associated with that process. Therefore sensitivity calculations must be run long enough to ensure convergence. This poses a particular problem for slow reactions such as O(¹D) + N₂O and slow lower altitude photochemistry that require run times approaching 5 years. We ensured that the time-dependent sensitivities were integrated to convergence. The vertical

transport time, which decreases from years at 20 km to weeks at 50 km (a true box model photostationary state), is a reliable clock for convergence of most steps. Furthermore, as we integrate the sensitivities to convergence we are required to maintain the steady solution of the particular box. This requires the inclusion of species source or sink terms resulting from the coupling of the boxes in the 2-D model, which has to be done in the least intrusive way to get meaningful sensitivities.

We extract parameters for instantaneous and localized parcels from the converged steady state 2-D LLNL output to construct the mechanism for the 0-D box sensitivity analysis. They include diurnal average values of rate constants, photolysis rates, and species concentrations for a specific altitude, latitude, and month. In addition, snapshots of production minus loss (P–L) rates for each species at each box are taken from the 2-D model. These rates ($\pm X \text{ cm}^{-3} \text{ s}^{-1}$) measure deviations of individual species from photostationary state, reflecting the transport effects and seasonal variations in long-lived species which couple the photochemistry of the various boxes in the 2-D model. The 0-D box mechanism uses the extracted diurnal average rate constants and photolysis rates. It includes pseudo-first-order source or sink steps for species (using dummy species) to balance the P–L terms to maintain the 2-D model solution, as the sensitivities are integrated to convergence. So, if the 2-D output shows an NO P–L rate of X/s , we add a pseudo-first-order loss rate for NO of $X/[NO]/s$. From a strictly local point of view, there are photochemical source terms for each of the families involved in catalytic ozone destruction: oxygen photolysis for O_x, O(¹D) + H₂O for HO_x, O(¹D) + N₂O for NO_x, CFC photolysis for ClO_x, and CH₃Br (plus CF₃Br and CF₂ClBr) for BrO_x. Unless 0-D loss rate steps (sometimes small) are added for each family, an excess of radicals will accumulate and ozone destruction will increase with time. The halocarbon species which photochemically decay are kept constant by inflating their abundance and reducing their photolysis and rate constants to keep the net rates the same. First-order source terms are added where necessary to maintain the concentrations of other long-lived stable species such as CH₄, H₂, CO, CH₂O, N₂O, and H₂O. Our 0-D box calculations begin with local diurnal average 2-D rate constant and species output specified as initial conditions, plus the necessary P–L make-up terms, and we then verify the absence of drifts in time from the local 2-D photochemical solution.

At a given location and season in the 2-D model, there are several reasons why a snapshot solution will drift when integrated in the box model without correction terms. Transport of various species from other locations of different photochemistry occurs on the convergence time scale, and even the local photochemical activity has sizable seasonal variations. Therefore the typical 2-D box is not in a local photostationary state. The size of this deviation can be computed for each species by totaling the sum of its production and loss rates, the P–L term, at the 2-D model location. If one adds an opposite kinetic source or sink term to counterbalance each P–L rate, a steady 0-D solution is ipso facto guaranteed. Ozone itself is typically not in stationary state in most 2-D model locales—we are after all looking at its sensitivity and time response as the main atmospheric photochemistry driver—and so an ozone P–L rate term in the box model is typically required if its concentration is to stay at the 2-D box value. As a consequence of this non-steady-state ozone value, we also typically see radical pairs active in the other photochemical families having large and opposite P–L terms which dominate the set of species P–L terms: NO and NO₂, OH and HO₂, Cl and ClO, and Br and BrO.

While the use of the complete set of individual P–L terms from the 2-D model output locks the 0-D Senkin solution to the particular 2-D box, it creates some artifacts that we had to eliminate. Specifically, the large radical P–L terms have high sensitivities that dampen the sensitivities for the photochemical sources and sinks of the radicals. For example, the NO and NO₂ radicals have large P–L rates in opposite directions that are primarily driven by the ozone P–L difference and the reaction NO + O₃ → NO₂ + O₂ that balance each other. Large absolute ozone sensitivities with opposing signs to large P–L terms for the couplets such as NO and NO₂ are evident in many simulations. Since these opposing P–L pairs (NO and NO₂, ClO and Cl, BrO and Br, and OH and HO₂) interconvert rapidly (<hours), summing their P–L rates to achieve substantial cancellation also maintains the same solution. We therefore adopted a summing of computed P–L terms for all species within a particular family (NO_y = NO + NO₂ + NO₃ + 2N₂O₅ + HNO₃ + HNO₄ + ClNO₃ + BrNO₃, Cl_y = Cl + ClO + 2Cl₂ + 2ClOOCl + HOCl + HCl + ClNO₃ + BrCl, and Br_y = Br + BrO + BrCl + HOBr + BrNO₃) that yields net family P–L terms several orders of magnitude lower than the largest individual terms. This net family rate is then used to compute a first order “makeup” rate to be applied to that member of the family having the largest P–L rate in the opposite direction, for use in the 0-D mechanism. This should represent the smallest perturbation to the 2-D mechanism. Since the photochemistry repartitions species within a family faster than the time scales for sensitivity convergence or net P–L adjustment, the net family approach is equivalent to using individual P–L terms and keeps our 0-D box at the 2-D solution (including within each family). The smaller net P–L terms also do not dampen the sensitivities to the photochemistry. We note that, unlike the LLNL 2-D model, almost all other 2-D models utilize this type of family based approximation to calculate short-lived species, transporting only the longer lived species, to speed up their calculations. The success of the family P–L approach in approximating the solution locally suggests that the large, fast, and opposite Cl and ClO P–L rates reflect the fact that O₃ itself is not in photostationary state and can be associated with the O₃ P–L term.

At some lower altitudes, it is necessary to include additional P–L species to prevent sizable drifts in the solution. Typically, a division between NO_x and NO_y is required—the sum of NO, NO₂, NO₃, and 2N₂O₅ is added for an NO P–L term and the remaining nitrogen family P–L sum gets assigned to HNO₃ removal. This is a particular problem below 25 km at 62N in Feb., where large opposite NO_x and NO_y P–L terms may perturb the sensitivity values. In some less active tropospheric boxes, large and opposite P–L rates are seen for the hydrocarbon oxidation intermediates CH₃OO and CH₃OOH, which are added and assigned to the larger term, and it is also occasionally necessary to use both OH and H₂O₂ P–L terms separately. Eventually, in those inactive regions where we present no solutions, only simulations approaching the full P–L method will succeed and offer hard-to-interpret results showing the very highest sensitivity to the P–L terms.

Seven atmospheric profiles from the model were examined: 2N Mar; 32N Mar; 47N Aug; 47N Feb; 62N Aug; 62N Feb; 78S Oct. As a general finding, locations above 40 km are in photostationary state, and the box model is an accurate representation. Above 20 km, the simple family P–L scheme works well in providing a frozen solution for sensitivity analysis with low ozone sensitivity to the P–L terms introduced. Significant P–L sensitivities and more complex P–L schemes

TABLE 1: Ozone Sensitivities and Changes at 25 km 47N Aug

reacn	S(O ₃)	k'/k	ΔO ₃ /O ₃
O + NO ₂	−0.327	1.129	−0.0397
OH + O ₃	−0.094	1.229	−0.0193
HO ₂ + O ₃	−0.084	0.808	0.0180
O + O ₂ = O ₃	0.471	1.031	0.0142
OH + NO ₂	0.090	0.897	−0.0098
(OH + NO ₂) ^a	0.090	(0.595)	(−0.0456)
NO + O ₃	−0.078	0.956	0.0035
HO ₂ + NO ^a	0.055	0.946	−0.0030
N ₂ O ₅ hydr	0.011	0.770	−0.0028
Cl + CH ₄	0.025	1.045	0.0011
Cl + O ₃	−0.027	1.039	−0.0010
NO ₂ + NO ₃	0.024	0.973	−0.0007
OH + HNO ₃	0.001	1.295	0.0004
total 94 to 00			−0.0391

^a JPL-97 change.

are often required for nontropical altitudes of 20 km and below, and high latitude winter results ≤25 km (78S Oct and 62N Feb) must be viewed with caution. Limited comparisons with results from 2-D model runs in which some of the sensitive rate constants were varied^{10,11} suggest that the various feedbacks in the 2-D model can dampen the 0-D model sensitivities at ≤25 km by a factor of 2 or more. Thus results presented here may overstate the effects of revised rate parameters at these altitudes.

Ozone Results

Our sensitivity results are based on outputs of the LLNL 2-D model using rate parameters from the NASA JPL-94 evaluation, with a few exceptions discussed later. Some 22 kinetic and photolysis recommendations to which our survey showed significant ozone sensitivity have changed, mostly in the JPL-2000 issue. Table 1 shows the predicted fractional ozone changes in decreasing rank order, computed by propagating rate constant changes via the sensitivities using eq 2, at one typical location. The first 5 reactions are responsible for the bulk of the changes predicted through most of the middle stratosphere, with the OH + HNO₃ rate constant increase also making a significant impact toward increasing the predicted ozone at 20 km and lower. The larger low-temperature value for O + NO₂ is the chief cause for expecting less stratospheric ozone using the new recommendations. It destroys odd oxygen catalytically and recycles NO₂ back to NO.

Noting effects of other rate constant changes, the HO_x–ozone adjustments largely cancel, but will change the OH/HO₂ ratios. Although only small adjustments were made to the recombination rate constant producing ozone, high sensitivities result in a significant impact. Changes in HOCl and HOBr photolysis were too small to influence predicted ozone, and the effects of a lower BrNO₃ cross section are compensated by the addition of a long wavelength tail to its spectrum. A change was also made to the heterogeneous hydrolysis of N₂O₅ by including a dependence on aerosol sulfate weight percentage. Sticking coefficients are near the old values of 0.1, and small effects will occur from the new treatment, except for lower ozone at some moist low altitude locations.

The JPL-97 changes introduced an even larger reduction in the OH + NO₂ rate constant at low temperature and pressure than the JPL-2000 recommendation, when compared to the JPL-94 values. (The JPL-2000 evaluation of nitric acid formation rate constants weights the data according to experimental uncertainty and incorporates two new investigations, whereas the JPL-97 result is largely due to the unweighted consideration of the available data.) Thus the parenthetical values in Table 1

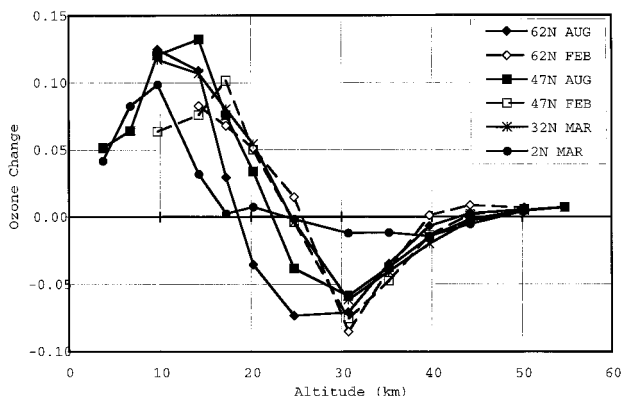


Figure 1. Predicted model ozone changes versus altitude at 6 latitudes (see key) as a result of recommended mechanism parameter changes in JPL-97 and JPL-2000, computed from the box model sensitivity coefficients.

show a much larger predicted ozone reduction for the JPL-97 value. The JPL-97 value overcorrects, and if one uses Table 1 to predict the effect of JPL-97 to JPL-2000 changes, the individual contributions cancel and no net ozone model change at 25 km 47N Aug. is predicted. (The comments on this reaction in JPL-2000 note a suggestion¹² of minor HOONO product at low temperature, which then decomposes. The net effect, as shown in ref 12, is to lower the effective OH + NO₂ rate constant back toward the JPL-97 value.)

Figure 1 shows the predicted model changes versus altitude at the various latitudes and seasons of our sensitivity survey. The middle stratosphere decrease in ozone illustrated for 47N in Table 1 is similar to behavior at other latitudes, except for the tropical location. The tropical region features considerable ozone production in the upper troposphere and lower stratosphere and strong upward ozone transport in the middle stratosphere. Thus ozone photochemical sensitivities and predicted changes are very small.⁶ We note from previous comparisons^{6,10} that the 0-D sensitivities may overestimate ozone changes for altitudes below 25 km, where transport coupling in the 2-D model becomes important and the P-L terms in the 0-D model become significant. Damping factors of 2 have been seen.

In general the results in Figure 1 predict up to 7% less ozone for the middle stratosphere and a 10% increase or more near the tropopause and upper troposphere. The rate parameter change most responsible for this ozone increase near the tropopause is the faster OH + HNO₃ rate, which removes ozone-destroying OH and produces NO₃ - a photolytic source of odd oxygen in the troposphere. The decrease in the rate constant for HO₂ destruction of ozone also leads to the higher ozone predictions in the upper tropospheric region, where HO_x not NO_x destruction of ozone is the dominant catalytic cycle. In the lower stratosphere HO_x levels are lowered by the rate changes and ClO_x is increasingly sequestered as ClONO₂ because NO_x is higher with the revised kinetics. These changes reduce the two most important catalytic ozone cycles in the lower stratosphere and tend to increase ozone. An exception can be noted for the high latitude 62N Aug location, where high photolysis rates enhance the contribution of NO_x catalysis to ozone loss in the lower stratosphere, and a 4% decline in ozone is predicted at 20 km as a result of the revised kinetics. This NO_x effect amplifies the spring to fall decline in lower stratospheric ozone at high latitudes and is consistent with recent observations and constrained box model studies.^{13,14} In the middle stratosphere the ozone is decreased by the increased NO_x, since the NO_x cycle dominates. In the upper stratosphere where NO_x chemistry plays a negligible role no changes in ozone

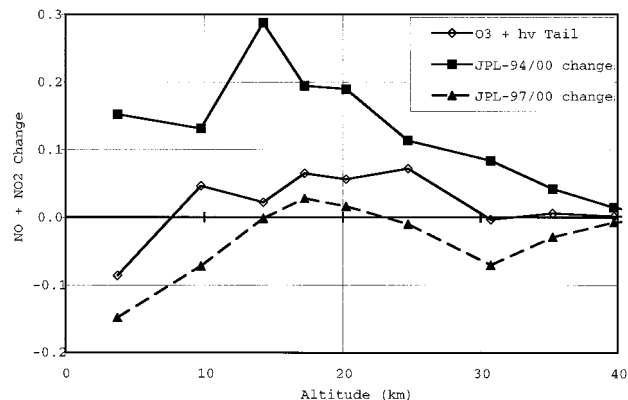


Figure 2. Predicted box model diurnal average NO_x changes versus altitude at 47N latitude in August as a result of mechanism parameter changes from JPL-94 to JPL-2000 (squares), from JPL-97 to JPL-2000 (triangles), and due to the addition of a long wavelength tail to O₃ + hv → O(¹D) from ref 15 (diamonds).

occur. The vertical ozone change profiles in Figure 1 clearly reveal this structure. Tables from the report⁶ are included in the Supporting Information which contain ozone sensitivities exceeding 0.01 at the analyzed locations, to permit similar analysis for future mechanism parameter changes or proposed changes and to provide a listing of the key reactions at various locations.

The conclusion that the JPL-2000 chemistry influences ozone significantly by enhancing NO_x has also been made in a recent constrained box model study.¹⁴ Bruhl and Crutzen demonstrate that the new rate parameters for O + NO₂, OH + NO₂, and OH + HNO₃ lead to a net decrease in column ozone. Our results are consistent with this finding and also support the conclusion that NO_x activation at mid-high latitudes is the main cause of the spring to fall decline in ozone in the Northern Hemisphere.

For the southern polar springtime location (not shown in Figure 1), negligible changes (<2%) in predicted ozone are computed above 20 km. Chlorine photochemistry dominates these sensitivities, and only small changes were recommended for these rate parameters. The exception occurs at 20 km, where $S = -0.35$ for the reaction HCl + ClONO₂ → Cl₂ on PSCs. A recommendation to increase this value leads to a predicted 20% decline in model ozone values from our analysis, although the model only provides an approximate representation of this location. The same analysis would apply to an increase in PSC surface area density. The negligible middle stratospheric changes might not apply to the northern polar regions (not examined here), due to complications from the availability of more NO_x from dynamical mixing or the effects of sporadic denitrification.

NO_x Results

Since the majority of rate parameter revisions influencing ozone involve nitrogen species, one may also expect changes in model NO_x/NO_y ratios. The sensitivity calculations also furnish coefficients for other species, and we have computed predicted changes in NO_x = NO + NO₂ at 47N in August as a function of altitude—as a simple sum given that total box model NO_y stays constant. We previously examined the effect of a OH + NO₂ ↔ HOONO channel (equivalent to reducing the OH + NO₂ → HNO₃ rate constant) on NO_x in a similar analysis.¹² The squares in Figure 2 show significant model NO_x increases are expected from the rate revisions of JPL-97 and JPL-2000. This is largely the result of a decrease in the HNO₃ formation rate constant and an increase in its destruction rate constant for reaction with OH. A secondary effect from the

TABLE 2: SST Ozone Perturbations at 47N June

altitude (km)	17.25	20.25	21.75	26.25
2-D LLNL model ΔO_3	-0.0078	-0.0143	-0.0151	-0.0130
0-D predicted $\Delta\Delta O_3$ (94 \rightarrow 00)	-0.0274	-0.0443	-0.0322	-0.0067
2-D estimated $\Delta\Delta O_3$	-0.0145	-0.0142	-0.0116	-0.0052
2-D uncertainty ^d	0.033	0.029	0.025	0.007

^d From ref 10; use of updated JPL-2000 uncertainties reduces values by only 20%.

increased OH + O₃ rate constant also contributes, since less OH is available to sequester NO_x via HNO₃ formation. Sensitivity analysis automatically accounts for such couplings.

The triangles show predicted NO_x model changes using the JPL-97 to JPL-2000 changes. Recall that the JPL-97 recommendation severely reduced the OH + NO₂ rate constant, so that raising this loss rate constant back up effectively counteracts the other JPL-2000 changes that increase NO_x. However, the cancellations are fortuitous and incomplete; while they apply in the local box model picture, somewhat different net changes may be experienced in a full 2-D model. These results suggest that diurnally averaged NO_x levels from models using JPL-97 kinetics could vary by up to 10% with the revised JPL-2000 values. Instantaneous changes under well illuminated conditions may be larger.

The predicted changes in both ozone and NO_x due to rate parameter revisions suggest assessment model predictions of effects of SST aircraft emissions on ozone levels may also change. We previously examined box model sensitivities at 47N for a June 2015 scenario featuring a fleet of 500 Mach 2.4 aircraft emitting 15 g of NO₂/kg of fuel at 18–20 km¹⁰ and derived kinetics uncertainties in these predictions using eq 3. (This is three times the emission level of the recent standard assessment scenario.^{1c}) The difference sensitivity is easily calculated from the individual logarithmic coefficients:

$$S_i(\Delta O_3) = S_i(O_3^*/O_3) = S_i(O_3^*) - S_i(O_3) \quad (4)$$

Then using eq 2 we can easily compute the expected change in local predicted ozone depletion due to the revised rate parameters.

The impact of rate changes from JPL-94 to JPL-2000 on predicted SST effects on ozone according to the box model sensitivities is shown in Table 2. ($\Delta\Delta O_3$ refers to the predicted change in the SST ozone perturbation due to the updated rate constants.) Increased ozone depletion by up to 4% absolute is indicated. Increased values for the O + NO₂ and OH + HNO₃ rate constants are chiefly responsible. However, some repeated 2-D model simulations performed for our SST uncertainty study¹⁰ suggest that the box model sensitivities will overstate effects in 2-D models by factors of 2–3 due to transport and seasonality effects. Applying these same damping factors leads to the predicted ΔO_3 changes in line 4, roughly doubling the depletions. These changes are about half the 2-D model kinetics uncertainty limits set in ref 10, shown in line 5. This expectation of significantly larger predicted ozone depletions leads us to recommend some additional assessment model simulations with the revised rate parameters. Given the dependence of SST ozone perturbations on the NO_y distributions assumed or computed, and the neglect of important transport considerations inherent in the 0-D sensitivity analysis, more quantitative conclusions are not warranted.

Effects of Other Changes on Ozone

Several other changes have been proposed in either the JPL-97 or JPL-2000 evaluations that deserve individual examination.

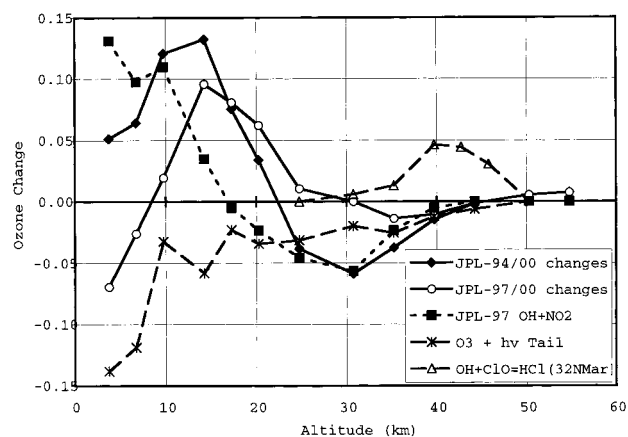


Figure 3. Predicted box model ozone changes versus altitude at 47N latitude in August as a result of specific mechanism parameter changes: \blacklozenge , changes from JPL-94 to JPL-2000; \circ , changes from JPL-97 to JPL-2000; \blacksquare , using $k(\text{OH} + \text{NO}_2)$ from JPL-97 instead of JPL-94; $*$, adding the long wavelength tail for $\text{O}_3 + h\nu \rightarrow \text{O}(^1\text{D})$ from ref 15; \triangle including a 7% yield for $\text{OH} + \text{ClO} \rightarrow \text{HCl} + \text{O}_2$ (computed for 32N latitude in March, from ref 11).

We look here at ozone changes at various altitudes at 47N in Aug with respect to the JPL-97 reduction in OH + NO₂, addition of a long wavelength tail to the ozone photolysis cross section for O(¹D) production, changes in the NO₃ photolysis branching fraction between O + NO₂ and O₂ + NO, and introduction of a OH + ClO \rightarrow HCl + O₂ channel. Aerosol loadings are also subject to change, and kinetic effects can be examined via the sensitivity coefficients for heterogeneous reactions.

As discussed in reference to Table 1 and Figure 2, the JPL-97 recommendation reduced the OH + NO₂ rate constant too much. The specific effect of that change from the JPL-94 value is plotted vs altitude in Figure 3 for 47N Aug. In the lower to middle stratosphere, the increase in available NO_x reduces ozone. In the troposphere, the extra NO₂ is a photolytic source of odd oxygen and a participant in “smog” chemistry. Figure 3 also plots for reference the effects on ozone of the changes from the JPL-97 to JPL-2000 rate changes. The cancellation of effects seen for NO_x in Figure 2 is also predicted for ozone in the middle stratosphere, but at lower altitudes significant changes are still predicted.

The JPL-97 evaluation also incorporates the addition of a long wavelength tail for ozone photolysis to form O(¹D) as advocated by Michelson et al.¹⁵ Since the LLNL 2-D model (and others) already incorporated this feature, we have treated this modification separately. The results shown in Figure 3 for 47N Aug are typical and were computed by taking the altitude dependent ratios of O(¹D) from Figure 3 of ref 15 as the values of $\delta k/k$ for the photolysis reaction. Since O(¹D) + H₂O initiates the HO_x destruction cycle of ozone, the predicted 5% lower ozone is not surprising. The values are approximate in that a rough estimate was used for $\delta k/k$ and no radiative or other multidimensional feedbacks are included in the box model sensitivity analysis.

The branching fraction for NO production from NO₃ photolysis was changed from 0.078 to 0.114 in the JPL-97 evaluation, on the basis of the measurements of Johnston et al.,¹⁶ essentially restoring the previous JPL-92 value. Since the LLNL model never used the lower yield, we considered this effect separately. Appropriate combinations of logarithmic sensitivity coefficients are easily assembled for other quantities, including branching fractions $A_1 = k_1/(k_1 + k_2)$.

TABLE 3: Sensitivities to Hydrolysis Reactions at 20 km 47N Aug

species	N ₂ O ₅	10× loading	BrNO ₃	10× loading
O ₃	-0.0347	-0.0225	-0.0120	-0.0584
OH	0.0891	0.0147	0.0354	0.0991
HO ₂	0.1626	0.0350	0.0375	0.0800
NO	-0.1775	-0.0708	-0.0198	-0.0372
NO ₂	-0.1981	-0.0854	-0.0289	-0.0840
ClO	0.2033	0.0599	0.0331	0.0516
BrO	0.0864	0.0141	0.0157	0.0162

Let $w = \delta(\ln k_1) = \delta k_1/k_1$. To keep the total $k_T = k_1 + k_2$ constant, $\delta(\ln k_2) = -(k_1/k_2)w$. Then $\delta(\ln A_1) = \delta A_1/A_1 = S_1 w - S_2(k_1/k_2)w$, and since w is also $\delta(k_1/(k_1 + k_2))$,

$$S(A_1) = S(k_1/(k_1 + k_2)) = S_1 - S_2 k_1/k_2 \quad (5)$$

Note that $S(A_2) = -k_1/k_2 S(A_1)$.

Using eqs 5 and 2, the predicted effect of the NO₃ photolysis branching fraction change on ozone is a decrease of 0.7–2% at 14–25 km for nonequatorial locations. The higher yield of NO leads to more ozone destruction and the lower yield of O + NO₂ leads to less ozone formation.

The JPL-2000 recommendation now includes a 7% branch for OH + ClO → HCl + O₂, which removes two ozone destroyers from the upper stratosphere, hence increasing predicted ozone. We do not compute sensitivities to missing reactions but did recently reanalyze some of our model boxes with this step added.¹¹ The resulting ozone changes for boxes at 32N Mar are also shown in Figure 3. Upper stratospheric ozone model increases of over 5% can be expected at higher latitudes.

One can also use the 0-D models of 2-D model boxes to examine effects and sensitivities to aerosol reactions and loadings. In nonpolar regions the heterogeneous processes are hydrolysis of N₂O₅, ClONO₂, and BrNO₃. At 20 km 47N in Aug, ozone and its key destroyer radicals are sensitive to the first and last, as shown in Table 3. For N₂O₅, we see that increased hydrolysis to HNO₃ reduces NO_x and secondarily increases the HO_x and ClO_x radicals. The largest effect is a redistribution of the controlling catalytic destruction cycles. We can also rerun the box models at 10 times the hydrolysis rates, i.e., 10 times the aerosol loading. The N₂O₅ sensitivities decrease dramatically as this reaction becomes saturated. Further incremental changes will have less effect, although of course the total rate of processing N₂O₅ has increased. But the sensitivity to BrNO₃ hydrolysis has now increased substantially, since it does not saturate even at high aerosol loading. Thus this type of analysis points to volcanically enhanced aerosol conditions at this sensitive location as an opportunity to examine bromine chemistry effects.

Ozone Photochemical Uncertainty

The JPL-2000 recommendations also significantly reduced several key reaction uncertainty values, which translates into a lower total photochemical uncertainty in model ozone, which we recompute here from the sensitivities. (JPL-94 results are in ref 6.) The relevant equation is

$$U(O_3) = (\sum(S_j \times \sigma k_j/k_j)^2)^{1/2} \quad (3)$$

where σk_j is the uncertainty in rate constant j . Reevaluated kinetics uncertainties have been lowered for 15 reactions that show significant ozone sensitivities, with sizable reductions for OH and HO₂ + O₃, and the recombination reactions forming

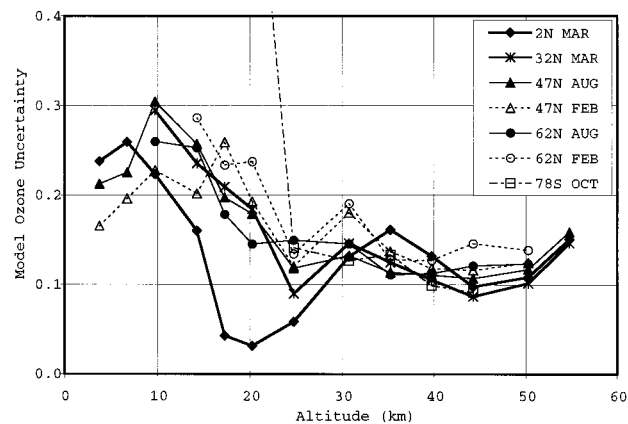


Figure 4. Uncertainties in model ozone versus altitude at 7 latitudes (see key) computed from the box model sensitivities using mechanism parameter uncertainties from JPL-2000 and excluding oxygen and ozone photolysis and reactions with O atoms.

O₃, N₂O₅, and ClONO₂. (Other reduced uncertainty reactions with significant ozone sensitivities are O and OH + HO₂, O + NO₂, OH + HNO₃ and HCl, O and BrO and ClO + ClO, Cl + CH₄, and BrNO₃ recombination.) For this analysis we focus on the kinetics and photolysis involving the catalytic ozone destruction cycles, radical coupling, and reservoir sink reactions. We exclude the consideration of oxygen and ozone photolysis and the reactions of O with O₂ and O₃. The results are plotted in Figure 4. Ozone uncertainties near 12% apply through most of the stratosphere. (Values using the higher JPL-94 kinetics uncertainties are about 3–5% larger.⁶) Ozone uncertainty in the lower stratosphere and troposphere cluster at about twice this level and more reactions contribute, although a cautious interpretation is warranted because the 0-D sensitivities may overestimate values for this region, where transport coupling in the 2-D model becomes important and the P–L terms in the 0-D model become significant.^{6,10} (See the previous discussion of damped sensitivities with respect to Table 2.) In the lower stratosphere the HO_x, NO_x, ClO_x, and BrO_x cycles are tightly coupled and many reactions are important in controlling ozone. Combining this with the large laboratory rate constant uncertainties at the extremely cold temperatures makes the lower stratosphere the region of highest local box model photochemical uncertainty. In the middle stratosphere ozone is principally determined by NO_x chemistry and only a few reactions are important. In the upper stratosphere the couplings between HO_x and ClO_x families increase the number of important reactions, but warmer temperatures mean higher confidence in the individual rate parameters. The critical reactions are identified in our report,⁶ and our conclusions on the relative importance of photochemical uncertainties in ozone predictions at various altitudes, latitudes, and seasons are consistent with Monte Carlo studies using the Goddard 2-D model.^{1a,17}

The equatorial region of low sensitivity and uncertainty to photochemistry is again evident. The ozone budget in the tropical region is dominated by ozone production and vertical transport by large scale advection, and this local photochemistry sensitivity analysis does not include feedback from transport and production terms. (We do include a sensitive O₃ P–L term that does reflect advection in tropics and suppresses local photochemical sensitivities.⁶) We also note the large rms ozone uncertainty of 65% for the Antarctic spring box at 78S Oct 20 km, which does not even include the additional 100% contributed by heterogeneous chlorine activation on PSCs. The many ClO and BrO reactions contributing to this sizable estimated

uncertainty suggest this is a good location for observational tests of these portions of the chemical mechanism.

It is important to note that these uncertainty estimates are from the kinetics measurements and assume no other knowledge beyond the laboratory rate measurements. They are unconstrained by atmospheric observations in agreement with model results, which do narrow the error limits on the combined kinetics of the mechanism.⁵ In addition, the lower stratospheric ozone sensitivities and uncertainties from the 0-D analysis may overstate the true 2-D values by a factor of 2 due to the effects of nonlocal feedbacks.¹⁰

Conclusions

The effects of recent photochemical parameter changes on model ozone calculations have been estimated using available box model sensitivity coefficients. Significant changes (5–10%) are predicted below the upper stratosphere, and revisions to the rate constants for $O + NO_2$, $OH + NO_2$, and $OH + HNO_3$ are chiefly responsible. These reactions also affect predicted NO_x levels. Since the analysis indicates an increase in model ozone depletion from SST emissions, it would be useful to recompute some assessment model simulations. Remaining ozone catalytic photochemistry uncertainties from the most recent evaluation imply a model ozone uncertainty of about 12% throughout the middle-upper stratosphere according to the sensitivity analysis results, with larger box model photochemical uncertainties of 25% in the lower stratosphere due to transport and chemical couplings and low-temperature kinetics uncertainties.

Acknowledgment. The sensitivity coefficient computations were supported by a grant from the Atmospheric Chemistry Program of the U.S. Department of Energy. We thank Ms. Natasha Greene for performing the initial sensitivity calculations of the polar region and Dr. W. Seth Hartley for computations of SST sensitivities. The work at LLNL was supported by the U.S. Department of Energy, under Contract W-7405-Eng-48. This work was performed while M.K.D. was at SRI International and D.E.K. was at LLNL. Support from LANL-NMRPI is also appreciated (M.K.D.).

Supporting Information Available: Tables of the ozone sensitivity coefficients at the sampled latitudes and altitudes for those reaction, photolysis, and P–L terms with sensitivities larger than 0.01. This material is available free of charge via the Internet at <http://pubs.acs.org>.

References and Notes

(1) (a) Stolarski, R. S.; Baughcum, S. L.; Brune, W. H.; Douglass, A. R.; Fahey, D. W.; Friedl, R. R.; Liu, S. C.; Plumb, R. A.; Poole, L. R.; Wesoky, H. L.; Worsnop, D. R. *1995 Assessment of the Atmospheric Effects of Stratospheric Aircraft*, NASA Ref. Publ. 1381; NASA: Washington, DC, 1995. (b) Douglass, A. R.; Carroll, M. A.; Demore, W. B.; Holton, J.

R.; Isakson, I. S. A.; Johnston, H. S.; Ko, M. K. W. *The Atmospheric Effects of Stratospheric Aircraft: A Current Consensus*, NASA Ref. Publ. No. 1251; NASA: Washington, DC, 1991. (c) Kawa, S. R.; Anderson, J. G.; Baughcum, S. L.; Brock, C. A.; Brune, W. H.; Cohen, R. C.; Kinnison, D. E.; Newman, P. A.; Rodriguez, J. M.; Stolarski, R. S.; Waugh, D.; Wofsy, S. C. *Assessment of the Effects of High-Speed Aircraft in the Stratosphere: 1998*; NASA Technol. Paper NASA/TM-1999-209237; NASA: Washington, DC, 1999.

(2) Johnston, H. *Science* **1971**, *173*, 517.

(3) (a) DeMore, W. B.; Sander, S. P.; Golden, D. M.; Hampson, R. F.; Kurylo, M. J.; Howard, C. J.; Ravishankara, A. R.; Kolb, C. E.; Molina, M. J. *Chemical Kinetics and Photochemical Data for Use in Stratospheric Modeling-Evaluation 10*; JPL Publication 92-20; Jet Propulsion Laboratory, California Institute of Technology: Pasadena CA, 1992. (b) DeMore, W. B.; Sander, S. P.; Golden, D. M.; Hampson, R. F.; Kurylo, M. J.; Howard, C. J.; Ravishankara, A. R.; Kolb, C. E.; Molina, M. J. *Chemical Kinetics and Photochemical Data for Use in Stratospheric Modeling-Evaluation 11*; JPL Publication 94-26; Jet Propulsion Laboratory, California Institute of Technology: Pasadena, CA, 1994. (c) DeMore, W. B.; Sander, S. P.; Golden, D. M.; Hampson, R. F.; Kurylo, M. J.; Howard, C. J.; Ravishankara, A. R.; Kolb, C. E.; Molina, M. J. *Chemical Kinetics and Photochemical Data for Use in Stratospheric Modeling-Evaluation 12*; JPL Publication 97-04; Jet Propulsion Laboratory, California Institute of Technology: Pasadena, CA, 1997. (d) Sander, S. P.; Friedl, R. R.; DeMore, W. B.; Golden, D. M.; Kurylo, M. J.; Hampson, R. F.; Huie, R. E.; Moortgart, G. K.; Ravishankara, A. R.; Kolb, C. E.; Molina, M. J. *Chemical Kinetics and Photochemical Data for Use in Stratospheric Modeling-Evaluation 13*; JPL Publication 00-03; Jet Propulsion Laboratory, California Institute of Technology: Pasadena, CA, 2000; <http://jpldataeval.jpl.nasa.gov>.

(4) Atkinson, R.; Baulch, D. L.; Cox, R. A.; Hampson, R. F.; Kerr, J. A.; Rossi, M. J.; Troe, J. J. *Phys. Chem. Ref. Data* **1997**, *26*, 521, 1329.

(5) (a) Wennberg, P. O.; Cohen, R. C.; Stimpfle, R. M.; Koplow, J. P.; Anderson, J. G.; Salawitch, R. J.; Fahey, D. W.; Woodbridge, E. L.; Keim, E. R.; Gao, R. S.; Webster, C. R.; May, R. D.; Toohey, D. W.; Avallone, L. M.; Proffitt, M. H.; Loewenstein, M.; Podolske, J. R.; Chan, K. R.; Wofsy, S. C. *Science* **1994**, *266*, 398. (b) Park, J. H.; Ko, M. K. W.; Jackman, C. H.; Plumb, R. A.; Kaye, J. A.; Sage, K. H. *NASA Models and Measurements Intercomparison II*; NASA/TM-1999-209554; NASA: Washington, DC, Sept 1999.

(6) Dubey, M. K.; Smith, G. P.; Kinnison, D. E.; Connell, P. S. *Rate Parameter Sensitivities and Uncertainties of a 2-D Stratospheric Ozone Model*; LLNL Report; Lawrence Livermore National Laboratory: Livermore, CA, 2000.

(7) Wuebbles, D.; Connell, P.; Grant, K.; Kinnison, D.; Rotman, D. In *The Atmospheric Effects of Stratospheric Aircraft: Report of the 1992 Models and Measurements Workshop*; NASA Ref. Publ. 1292; Prather, M. J., Remsberg, E. R., Eds.; NASA: Washington, DC, 1993; Vol 1.

(8) Kohlmann, J.-P.; Bluhm, H.; Poppe, D. *Atmos. Environ.* **2000**, *34*, 2451.

(9) Lutz, A. E.; Kee, R. J.; Miller, J. A. *SENKIN: A Fortran Program for Predicting Homogeneous Gas-Phase Chemical Kinetics with Sensitivity Analysis*; Report SAND87-8248; Sandia National Laboratories: Albuquerque, NM, 1988.

(10) Dubey, M. K.; Smith, G. P.; Hartley, W. S.; Kinnison, D. E.; Connell, P. S. *Geophys. Res. Lett.* **1997**, *24*, 2737.

(11) Dubey, M. K.; McGrath, M. P.; Smith, G. P.; Rowland, F. S. *J. Phys. Chem.* **1998**, *102*, 3127.

(12) Golden, D. M.; Smith, G. P. *J. Phys. Chem.* **2000**, *104*, 3991.

(13) Fahey, D.; Ravishankara, A. R. *Science* **1999**, *285*, 208.

(14) Bruhl, C.; Crutzen, P. J. *J. Geophys. Res.* **2000**, *105*, 12163.

(15) Michelson, H. A.; Salawitch, R. A.; Wennberg, P. O.; Anderson, J. G. *Geophys. Res. Lett.* **1994**, *21*, 2227.

(16) Johnston, H. S.; Davis, H. F.; Lee, Y. T. *J. Phys. Chem.* **1996**, *100*, 4713.

(17) Stolarski, R. S. Personal communication, 2000.